# IDENTIFICATION OF THE LOCATION PHASE SCREEN OF ERS-ENVISAT PERMANENT SCATTERERS

**M. Arrigoni[(1)], C. Colesanti[(1)], A. Ferretti[(2)], D. Perissin[(1)], C. Prati[(1)], F. Rocca[(1)]**

*[(1)] Dipartimento di Elettronica e Informazione, Politecnico di Milano,*
*Piazza L. da Vinci, 32 -20133 Milano, Italy, Phone: +39-02-23993697,*
*Fax: +39-02-23993413, E-mail: perissin@elet.polimi.it*
*[(2)] Tele-Rilevamento Europa - T.R.E. S.r.l., Via V. Colonna, 7 -20149 Milano, Italy*

## ABSTRACT

The phase time series of a point-wise Permanent Scatterer shows an additional phase shift passing from ERS to ENVISAT. This shift depends both on the existing 30MHz frequency shift between ERS and ENVISAT and on the location of the PS within the slant range resolution cell. The phase shift changes from one PS to another, but it is constant for all the ENVISAT images and is called "location phase screen" . In this presentation we show the experimental evidence of its existence. A data set of 90 ERS images and 7 ENVISAT images (ERS-like mode) on Milano has been used. Moreover, the location phase screen can be exploited to combine coherently ERS/ENVISAT SAR images and to identify the precise location of the Permanent Scatterers.

## 1 ERS AND ENVISAT INTERFEROGRAMS ON PS's

A key difference between ERS and ENVISAT SAR images is the 30 MHz central frequency change from 5.3 to 5.33 GHz. This change entails advantages as well as disadvantages: classical interferometry on distributed scatterers is made impossible, unless the normal baseline ranges from –1000 m to – 3000 m [1], [2], [3] so that the wavenumber shift ensures sufficient range common band.

In the case of point scatterers (or at least scatterers with a reduced slant range extension) the baseline range allowing for a prediction of the phase signature from the ERS to the ENVISAT operating frequency is extended and cross-interferograms can be created without strict constraints on the normal baseline. In fact point scatterers are imaged coherently with both systems by definition. Their phase histories can be combined moving from one to the other frequency. Of course this requires the correction of the deterministic phase term depending on the scatterer position coupled with the normal baseline and the frequency shift.
In fact, the phase shift due to the change of frequency from $f_0$ to $f_0+\Delta f$, for a given PS with slant range position and elevation respectively $\Delta r$ and $\Delta q$ (both relative to the center of the sampling cell taken as origin of the coordinates) is:

$$\Delta\phi = \frac{4\pi}{c}\left\{\Delta r\Delta f + \Delta r\frac{f_0 B_n}{r_M \tan\theta} + \Delta q\frac{f_0 B_n}{r_M \sin\theta}\right\} \quad \textbf{(1)}$$

where $c$ is the light speed, $B_n$ the normal baseline, $r_M$ the sensor-target distance and $\theta$ the incidence angle.
Besides the flat Earth and topography phase terms a new contribution depending on the frequency shift and on the slant range position of the point-wise target arises. Given the 30 MHz frequency variation, the phase change across a slant range resolution cell amounts to about $4\pi$. Therefore, (besides the exact elevation) the location of the scatterer within the cell has to be known with about 1 m precision, to be able to predict its phase within one radian. On each ERS-ENVISAT cross-interferogram a Location Phase Screen (LPS) will be superimposed (in correspondence of the PS). The LPS is uncorrelated in space but is the same in all cross-interferograms since both the PS slant range position and the frequency shift are constant. As a matter of fact the LPS values in the cross-interferograms at PS's will yield the PS positions within the resolution cell.

## 2 DC VARIABILITY

Since June 2001 ERS-2 operates in Zero Gyro Mode (ZGM), reducing the attitude control and causing DC values to exceed often the interval +/- 0.5 PRF. Conventional interferometry is no longer feasible on a systematic basis. In fact, both a DC estimate with ambiguity resolution and an azimuth common band filtering become mandatory for generating

*Proc. of FRINGE 2003 Workshop, Frascati, Italy,*
*1 – 5 December 2003 (ESA SP-550, June 2004) 45_prati*

conventional interferograms. Nevertheless, simultaneous constraints both on DC and normal baseline reduce significantly the number of images suitable for conventional interferometry.
For what concerns PS's, as long as their size is sufficiently smaller than the azimuth sampling cell, only a negligible amount of decorrelation is introduced whereas an additional deterministic phase term reflecting the PS position along azimuth arises, similarly to what happens for the frequency shift. Simple trigonometry yields:

$$\varphi_{AzPos} = \frac{4\pi}{\lambda}\Delta x\left(\tan\gamma_{master} - \tan\gamma_{slave}\right) \approx 2\pi\frac{\Delta f_{DC}}{PRF}\frac{\Delta x}{\delta_{az}} = 2\pi\Delta f_{DC,\,norm}\Delta x_{norm} \qquad \textbf{(2)}$$

which highlights an interferometric phase term dependent on the difference of the Doppler Centroid value from the Master to the Slave acquisition and on the actual azimuth position of the point-wise radar target with respect to the center of the corresponding azimuth sampling cell (i.e. the sampling position).
From this point of view, the Doppler Centroid frequency variability allows to locate an object in the azimuth dimension as well as the ERS-ENVI frequency shift gives the possibility to find it in the slant range direction, and an azimuth LPS at PS's can be found, similar to the one in range.

## 3 FIRST RESULTS

A data set of 90 ERS images and 7 ENVISAT images (ERS-like mode) on Milano over an urban frame of 2 km$^2$ has been used. ENVISAT images have been registered on the sampling grid of the ERS master image and ERS-ENVISAT interferograms have been generated with reference to the unique ERS Master (taking into account the different wavelengths and the ERS DEOS and ENVISAT DORIS precise orbits). As reference a very good PS ($|\gamma|_{ERS}$ >0.97) has been chosen. Its noise has been estimated and compensated.

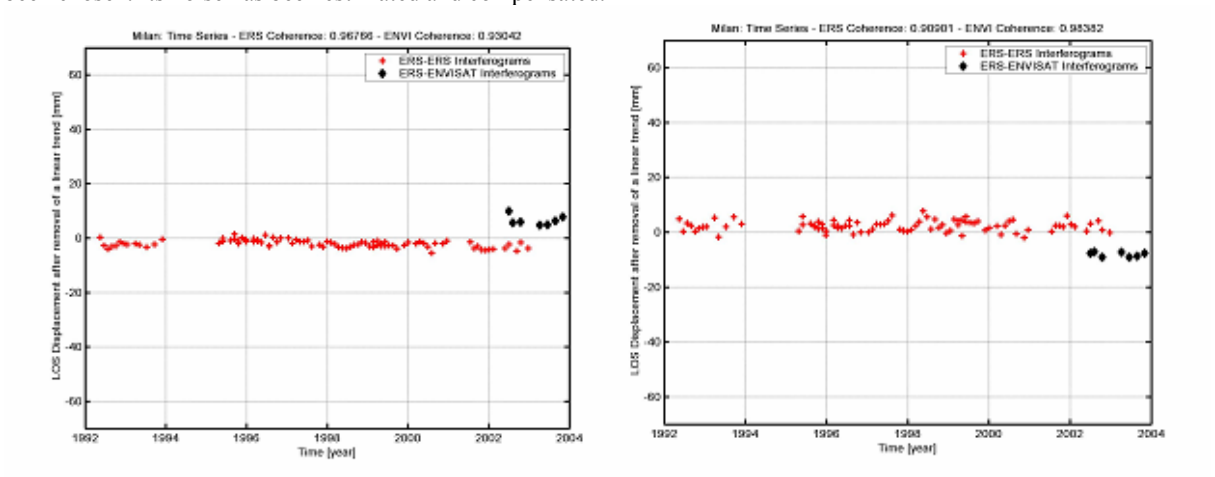


Figure 1: Examples of ERS-ENVI time series.

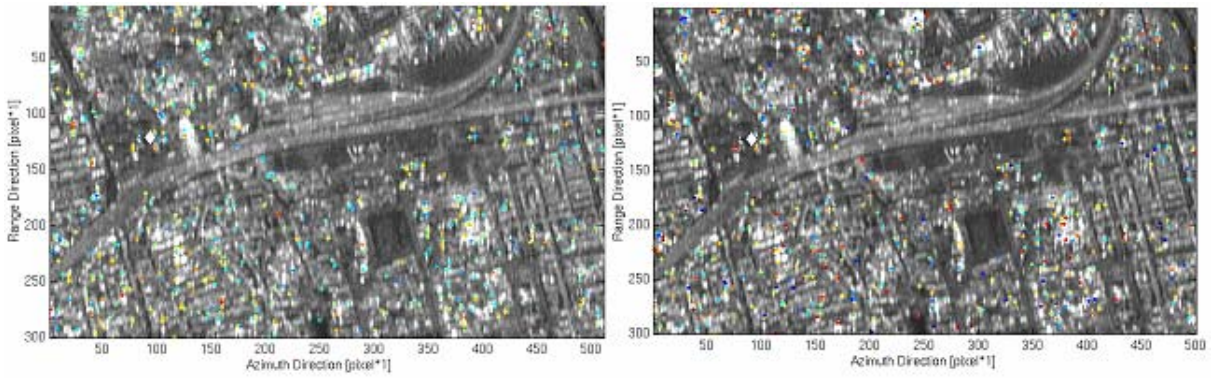


Figure 2: Azimuth and range Location Phase Screen.

Starting from the results of the PS analysis carried out on ERS data alone ($|\gamma|_{ERS}$, exact elevation, average LOS deformation rate), the topographic and deformation phase terms at PS's are removed from ERS-ENVISAT interferograms. Due to the limited extension of the test area, when working on phase differences, relative to close ERS PS's, we can estimate the effect of atmospheric disturbances (Atmospheric Phase Screen, APS) evaluating the phase residuals after compensating for the terms above.
Figure 1 shows two examples of ERS-ENVI time series, after subtraction of deformation, topography and atmosphere effects. The phase shift depending on the frequency shift is evident, and figure 2 reports both the azimuth and range LPS.

## 4 INCOHERENT APPROACH

Of course it is possible also to perform an incoherent combination of the ERS PS time series with ENVISAT data generating only ERS-ERS and ENVISAT-ENVISAT interferograms. Two distinct Master images (an ERS and an ENVISAT) are used, leading actually to two distinct time series. Usually this leads again to a constant offset between ERS-ERS and ENVISAT-ENVISAT data, even though this phase jump has no physical interpretation.

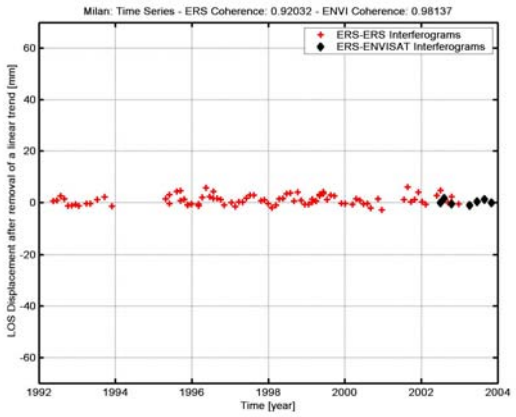


Figure 3: Incoherent time series.

## 5 ERS-ENVI POPULATION

How many ERS-PS's are still coherent in ERS-ENVI interferograms? Figure 4 shows that more than 80% of PS's with ERS-coherence greater than 0.9 stay permanent; the same applies to about 70% of those with $|\gamma|_{ERS}$ greater than 0.8. This proves that most targets are capable of guaranteeing continuity between ERS and ENVI time series.

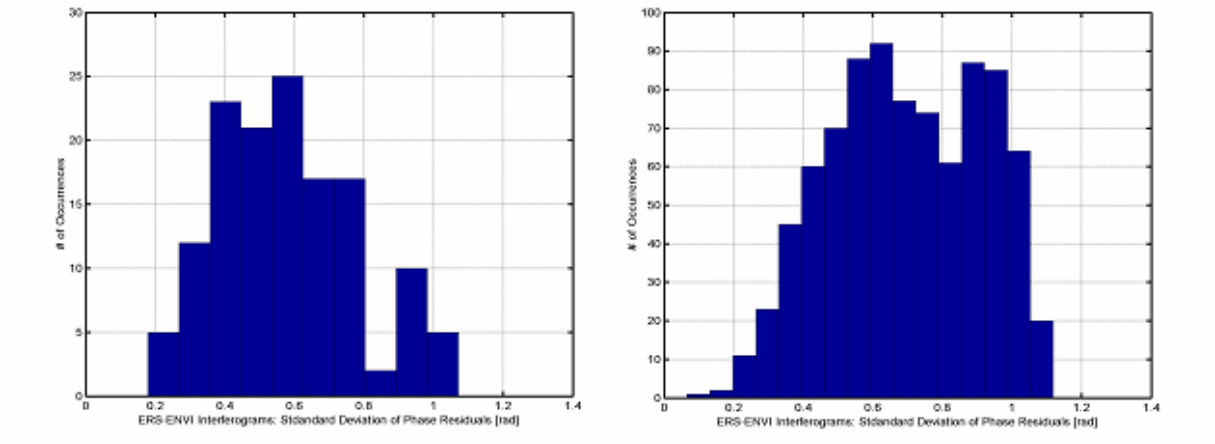


Figure 4: Phase residual standard deviation histograms, for PS with $|\gamma|_{ERS}$>0.9 (left) and $|\gamma|_{ERS}$>0.8 (right).

## 6 GEOMETRICAL CHARACTERISTICS ESTIMATION

Which targets are behaving as PS both in ERS-ERS and in ERS-ENVI interferograms? The answer to this question refers to a geometrical problem. A point-wise object appears the same for every angle of view, but a more complex one (e.g. something wider) can lose coherence if observed beyond a given geometrical threshold. Is it possible to gain information on the target shape from SAR data in C-band? Or, more generally, what are indeed Permanent Scatterers?
Three different strategies have been chosen to tackle the problem, and here some preliminary results are reported.
The focused radar signal amplitudes have been observed, searching for a deterministic dependency on the acquisition geometry. A systematic observation of PS's superimposed on orthorectified photos has been started, together with some in situ surveys. Finally, an example of target response has been simulated, in order to find a correspondence with the observed data.

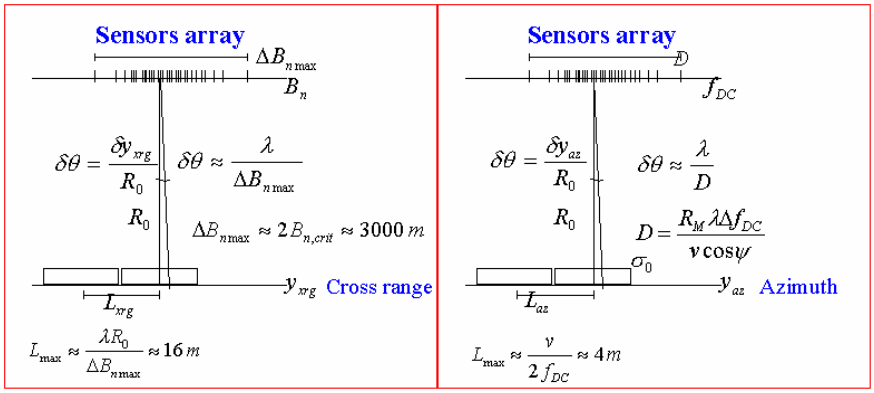


Figure 5: Acquisition geometry referred to the master image.

In figure 5 the acquisition geometry referred to the master image is seen as a sensors array in azimuth and in cross-range directions. The system resolution capability can be computed referring to the well known DOA theory. The minimum ground distance between two wave sources that permits to see them separated corresponds to the width of an object whose Fourier transform main lobe covers exactly the array extension. A wider target would have a thinner main lobe, thus a minimum would be seen by the array sensors, and it couldn't behave as a permanent scatterer. On the other side, a point-wise scatterer shouldn't show any amplitude dependency upon the sensor position.
Indeed, some curvatures and slopes of the amplitudes as a function both of the normal baseline and of the Doppler Centroid frequency have been seen. It is possible to read them as a measure of the object dimensions in cross-range and in azimuth, under the hypothesis of uniform surface scattering. In this case, the amplitude response in the transformed dominions can be modelled as a cardinal sine.

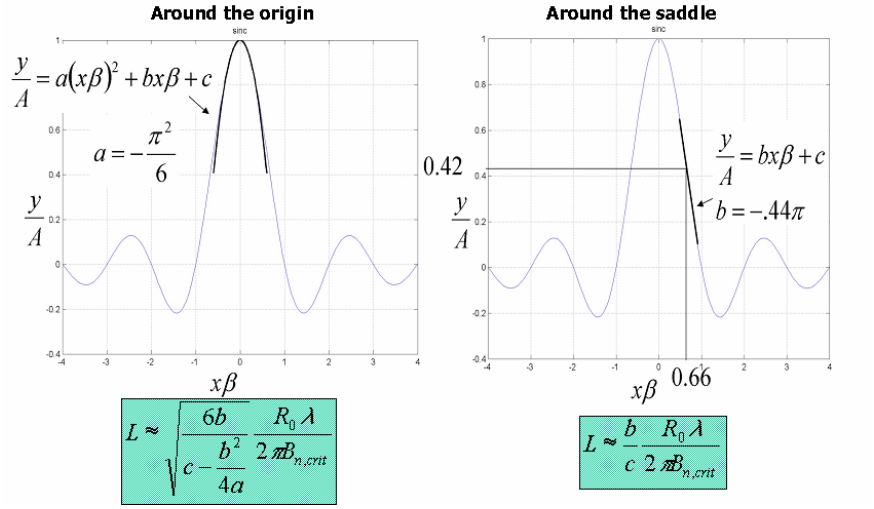


Figure 6: Cardinal sine parameters estimation.

Thus the problem is reduced to the estimate of the three cardinal sine parameters (main lobe width $\beta$, maximum amplitude $A$ and x-axes shift $x_0$) from a non uniform windowed set of samples.

$$y(x)=A\,\mathrm{sinc}(\beta(x-x_0))+n \tag{3}$$

Three equations yielding the value of the cardinal sine and its two first derivatives in $x_0$ can be exploited.
The curvature could be estimated only in correspondence of the cardinal sine maximum, and the slope in correspondence of the first saddle (figure 6 and 7). An error on this approximation yields to a width overestimation.

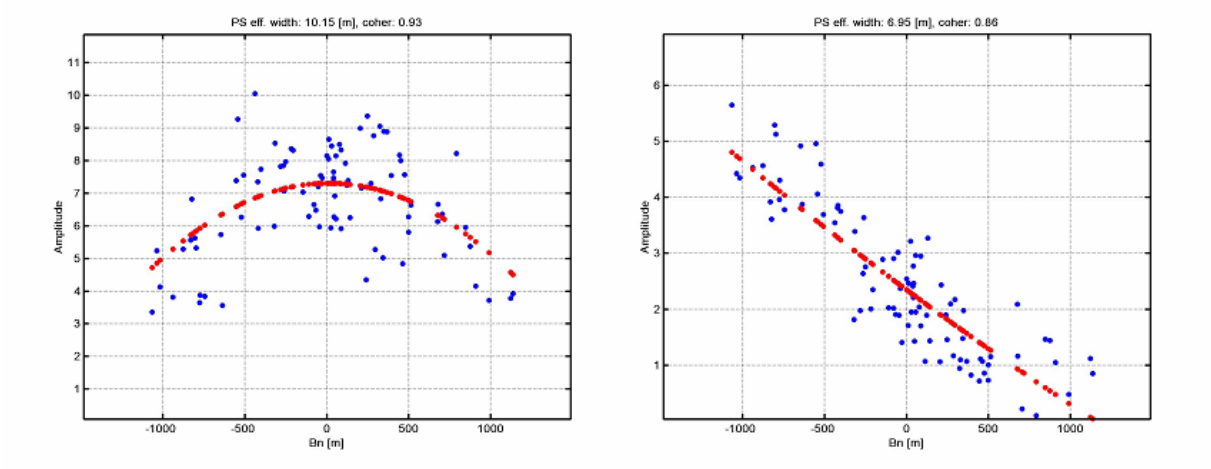


Figure 7: Examples of amplitude dependency on the normal baseline.

Looking at the baseline and Doppler value distribution, it should be noted that the Doppler set is not yet a sufficient statistic. Thus, the amplitudes azimuth dependency has been taken into account in order to better control the variation with respect to the baseline, but at the moment no azimuth width estimate has been carried out.
Preliminary results over an urban area in Milan show that 3% of PS's have a curvature and 8% have a slope. In figure 8 the histograms are reported of the corresponding width estimate in case of surface scattering. The remaining PS's do not show either a curvature or a slope. This means that their cross-range extension must be smaller than 1 m.

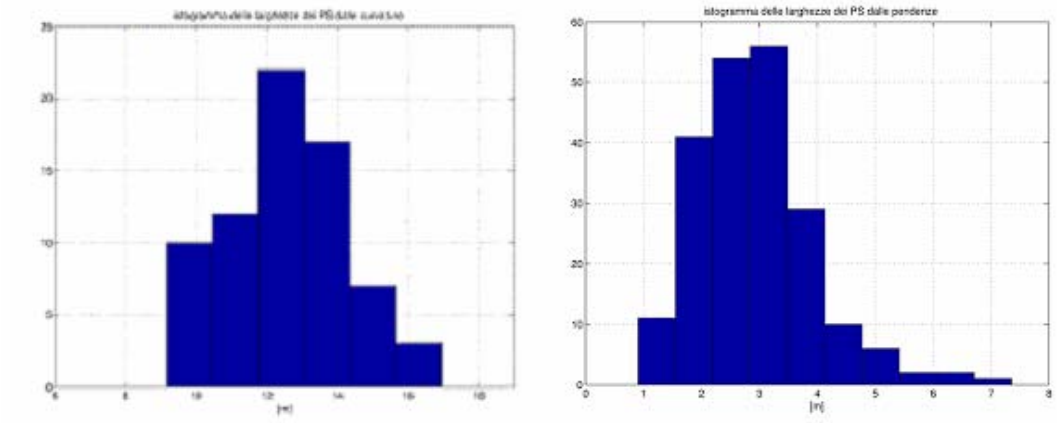


Figure 8: Cross-range width histograms got from amplitudes curvatures (l), or slopes (r).

## 7 ANALYSIS "IN SITU"

Which objects should appear smaller than 1 m? A possible answer comes from the observation of the orthorectified photos. Clear examples of a dihedral with at least some cylindrical symmetry (i.e. something that, given a nominal incidence angle, has a constant response notwithstanding the change of the look angle) are poles on flat scattering

planes. In figure 9 an easily recognizable example is reported, i.e. poles on tennis courts. They appear as PS's even if they have small radar cross section, because no clutter affects the radar signal.
A simulation of the structure composed by a cylindrical iron rod in vertical position on a flat terrain shows which pole dimensions and contour conditions make it a permanent scatterer.
Figure 10 shows a more complex example: a set of PS's on a fence oriented $66^0$ with respect to the azimuth direction.

Figure 9: Pole on tennis courts (l, c), pole simulation (r).

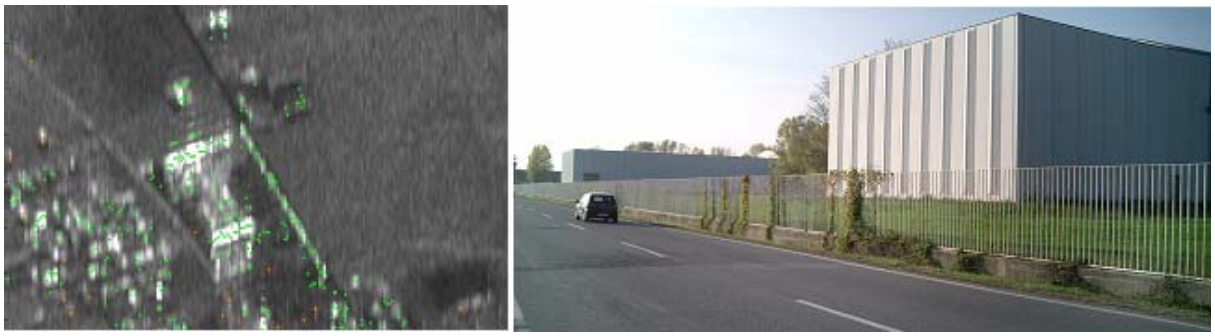

Figure 10: PS's on a fence.

## 8 CONCLUSIONS

The frequency shift between ERS and ENVISAT can be exploited in order to gain information on the slant-range sub-cell positioning of a Permanent Scatterer. In addition to the positioning capability due to the baseline and Doppler Centroid observation set, this yields the possibility to identify the location of a PS within a 1-meter cube.
Moreover, the percentage of ERS-PS's that keep on being stable in ERS-ENVI interferograms, states the historical continuity of the time series, giving the possibility of long term interferometry from 1991, allowing to measure very slow earth motions on a pixel by pixel basis in a unique coherent time series.
Not all PS's seem to be point-wise, as their amplitude behaviour as a function of the acquisition geometry demonstrates. A way to find an equivalent width of a small set of PS's has been shown. Most, like poles, have flat response, and this means that their effective cross-range extension is smaller than 1 m.
Further activity is expected to validate the signal geometrical dependency interpretation, to carry on in situ surveys and to analyse the noise sources on the amplitudes.

**References:**


[1] F. Gatelli et al., "The Wavenumber Shift in SAR Interferometry", IEEE TGARS, Vol. 32, no. 4, 1994.

[2] N. Adam, "Das erste Cross-Interferogramm aus Aufnahmen der Radarsensoren ENVISAT/ASAR und ERS-2"

[3] A. Monti Guarnieri, C. Prati, "ERS-ENVISAT Combination for Interferometry and Super-resolution", ERS-ENVISAT Symposium (Gothenburg, Sweden), 1222 October, 2000.